Materials Research. 2014; 17(Suppl. 1): 15-22
DOI: http://dx.doi.org/10.1590/S1516-14392014005000044
© 2014

Polymorphism of $CaCO_3$ and Microstructure of the Shell of a Brazilian Invasive Mollusc (*Limnoperna fortunei*)

***Arnaldo Nakamura Filho*[a,b]*, *Arthur Corrêa de Almeida*[a,b], *Hérnan Espinoza Riera*[a,b],**

***João Locke Ferreira de Araújo*[b], *Vitor José Pinto Gouveia*[c],**

***Marcela David de Carvalho*[d], *Antônio Valadão Cardoso*[a,b,c]**

[a]*Rede Temática em Engenharia de Materiais – REDEMAT, Ouro Preto, MG, Brazil*
[b]*Centro de Bioengenharia de Espécies Invasoras de Hidrelétricas – CBEIH, Belo Horizonte, MG, Brazil*
[c]*Fundação Centro Tecnológico de Minas Gerais – CETEC, Belo Horizonte, MG, Brazil*
[d]*Companhia Energética de Minas Gerais – CEMIG, Belo Horizonte, MG, Brazil*

Received: June 19, 2013; Revised: January 30, 2014

Applying the theories of Materials Science and Engineering to describe the composition and hierarchy of microstructures that comprise biological systems could help the search for new materials and results in a deeper insight into evolutionary processes. The layered microstructure that makes up the freshwater bivalve *Limnoperna fortunei* shell, an invasive specie in Brazil, was investigated utilizing SEM and AFM for the determination of the morphology and organization of the layers; and XRD was used to determine the crystalline phases of the calcium carbonate ($CaCO_3$) present in the shell. The presence of the polymorphs calcite and aragonite were confirmed and the calcite is present only on the external side of the shell. The shell of *L. fortunei* is composed of two layers of aragonite with distinct microstructures (the aragonite prismatic layer and the aragonite sheet nacreous layer) and the periostracum (a protein layer that covers and protects the ceramic part of the shell). A new morphology of the calcite layer was found, below the periostracum, without defined form, albeit crystalline.

Keywords: *microstructure, Limnoperna fortunei, SEM, AFM, XRD*

1. Introduction

$CaCO_3$ is the second most abundant mineral existing in the earth's crust, exceeded only by quartz. Crystalline $CaCO_3$ occurs in three forms: calcite, aragonite and vaterite. $CaCO_3$ also occurs in amorphous phase (ACC – amorphous calcium carbonate). Calcite is the most abundant, crystallizes according to the triclinic system and possesses a density of 2.71g/cm^3. Bridgman was the first to show that calcite has high-density polymorphic forms[1]. Much less abundant than calcite is aragonite, an orthorhombic polymorph having a density of 2.93g/cm^3. The third polymorph is vaterite, hexagonal and with a density of 2.54g/cm^3. Aragonite and vaterite are metastable at normal ambient temperatures[2].

One of the most fascinating aspects of biomineralization is the nucleation and maintenance of metastable phases at physiological temperatures. Due to the ability of the organisms to control the chemical conditions at nucleation sites, an "ionic pressure" enables the permanence of metastable phases under conditions that would normally preclude their maintenance. In the shell of bivalve, mainly made of calcium carbonate ($CaCO_3$), calcite and aragonite are the prevalent forms, but there are also highly unstable amorphous phases (ACC)[3]. These polymorphic transitions of $CaCO_3$ are classified as of second order, like the temperature of glass transition (Tg) of amorphous materials, and would represent an intermediate case between transformations of the displacive type (of the type beta quartz - alpha quartz) and order-disorder transitions (amorphization)[4].

The shells act as skeletons for supporting the soft parts of the molluscs' body, offer mechanical protection against predators and, in terrestrial species, keep abrasive materials (earth and sand) out of the mantle cavity[5]. They are composite organominerals (biominerals), constituted of nearly 95% $CaCO_3$ and 5% proteins and polysaccharides. Different taxonomic groups have different microstructures composed by varied morphological and structural arrangements, derived from polymorphic phases of calcium carbonate. Environmental pressures select more efficient structures and manufacturing processes. The Materials Engineering lend to Biology its knowledge and tools, assisting in the search for understanding how biological materials affect the survival of organisms[6-12].

The *Limnoperna fortunei*, or golden mussel, is a freshwater bivalve, native to Southeast Asia. This mussel was inadvertently introduced into South America by means of the ballast water of commercial vessels[13]. The impacts caused by the mussel have been reported in natural and artificial environments. Blocking of pipes, turbines and obstructions in water treatment plants are the consequences that are the most costly to repair. Impacts

*e-mail: nakamuraaf@gmail.com

on the natural populations can be irreversible causing rapid transformation in the communities of benthic macroinvertebrates[14,15].

The objective of this study was to characterize the microstructures and to determine the calcium carbonate phases present in the shell of *L. fortunei* to help to understand the processes involved in the formation of the shell (biomineralization), aiming to promote the creation of new controlling methods this invasive specie.

2. Methods

Golden mussel adults were collected in the River Paranaíba, Municipality of São Simão (lat.19,588611/ long. 50,980000) in the State of Goiás, in the middle of December 2010 (spring/summer) and transported in refrigerated and aerated boxes to the CETEC laboratory in Belo Horizonte - MG.

In the laboratory, seven animals with a length between 15 mm to 25 mm were collected randomly, euthanized humanely and extracted from the shells with tweezers and scalpel totalizing 14 shells. The shells were carefully washed with deionized water and kept in 70% alcohol until the preparation for scanning electron microscopy, atomic force microscopy and X-ray diffraction.

The shells were kept separately so that the shells of the same animal were not analyzed by the same technique and distributed as follow: Seven (7) shells were destined to SEM analysis, two (2) shells to AFM and five (5) shell to XRD. Golden mussels do not have sexual dimorphism, so the determination of the gender requires specific techniques that were not used in this work.

2.1. *Scanning electron microscopy*

The preparation of the samples for scanning electron microscopy was done at the Centre of Microscopy of the Universidade Federal de Minas Gerais - UFMG. The shells were carefully washed with deionized water and dried at room temperature. After drying, shell samples were mechanically fragmented and random pieces were fixed to the sample holder with the help of carbon ribbon and silver paint, so that it was possible to visualize the fragments transversally. Seven (7) shells collected on the same day and in the same place, but presenting different sizes were used. The samples were not metallized. The electrons were conducted through the carbon ribbon and the silver paint. The scanning electron microscope used (SEM) was the Quanta 200 model (FEG – FEI) operating under varied conditions to obtain the best images (the conditions are all specified in the SEM micrographs).

2.2. *Atomic force microscopy*

The topography of the layers was measured using Veeco Dimension V Atomic Force Microscopy (AFM). Measurements were performed in air, in tapping mode, using a Si probe with cylindrical tip of 6nm radius. Before AFM scanning, two shells samples from different animals were cleaned and embedded in resin (polyester resin SR 102 for industrial use), cut and polished down to allow transverse viewing of the layers.

2.3. *X ray diffraction*

For the determination of the $CaCO_3$ (calcium carbonate) phases that make up the shell, tests were carried out using an X ray diffractometer (XRD-6000 Shimadzu) with horizontal goniometer (θ-2θ).

Shells of *L. fortunei* were carefully washed with deionized water and brush, dried at ambient temperature. Tests were carried out on shell powder (with periostracum), ground with a pestle and mortar, and on the whole shells.

Tests were carried out on the internal and external (dorsal and ventral) regions of the shell (Figure 1 – a, b and c respectively) in addition to the powder. The diffraction patterns obtained were compared with the calcite (card# 83-578) and aragonite (card# 76-606) cards from crystallographic records of the International Center for Diffraction Data (ICDD) database, available with the equipment software. Quantitative analyses of the phases were not carried out.

3. Results and Discussion

The scanning electron micrographs of the bivalve's shell permitted the identification of 4 (four) layers and the X-ray diffraction identified 2 (two) polymorphs of $CaCO_3$ – calcite and aragonite – located in different regions of the shell.

3.1. *Scanning electron micrographs*

The transverse visualization of the shell fragments made possible the identification of four (4) layers that make up the shell of the *L. fortunei* (Figure 2). From the external layer to the internal layer of the shell are – the periostracum, which is the first layer secreted by the folds of the mantle and is composed of proteins. Below the periostracum have a layer without a defined form composed of calcite named as "Calcite Cloud Layer". Following that is the aragonite sheet nacreous layer - which occupies nearly the whole thickness of the shell - and finally the aragonite prismatic layer.

In Figure 3 the periostracum (≈7μm), is shown, which is composed of a proteic sclerous double layer (external

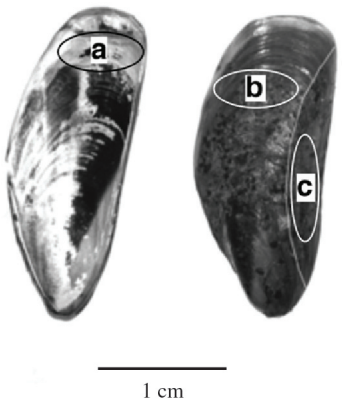

Figure 1. Photography showing the regions where X-Ray Diffraction tests were carried out. a – internal region, b – external dorsal region and c – external ventral region of the shell of the *L. fortunei*. Bar = 1 cm.

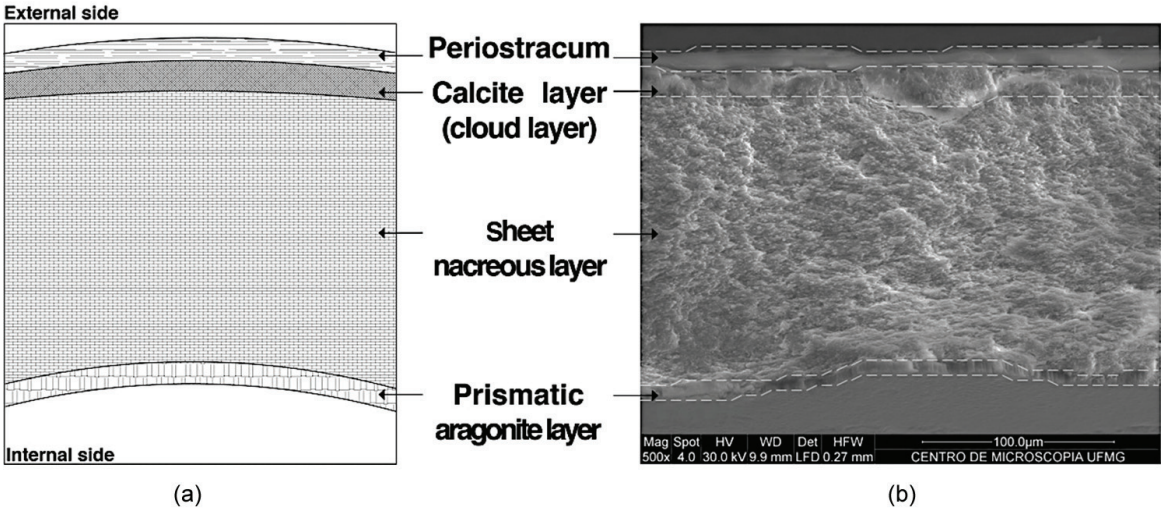

Figure 2. (a) – schematic draw and (b) SEM micrograph of a transverse section of the *L. fortunei* 's shell showing the layers and how they are organized; upper part is the outside of the shell and lower part is the internal side; in sequence: periostracum, proteinic layer that covers and renders the shell impermeable; calcite layer without defined microstructure; aragonite sheet nacreous layer and aragonite prismatic layer. In the image on the right the dashed lines represent the limits between the shell layers. Bar = 100µm.

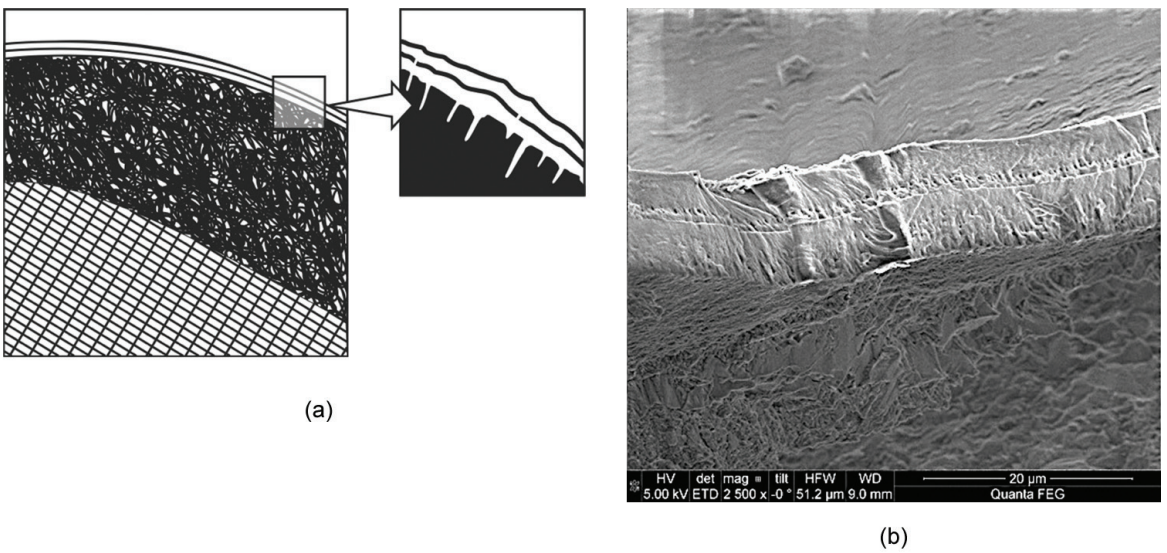

Figure 3. (a) – Schema showing the double layer of the periostracum, a proteinic layer that covers the shell on the outside. It renders the shell impermeabilizing and protecting the ceramic layers below. The white area between black lines is the periostracum, the black area is the calcite cloud layer and the gridded area is the sheet nacreous layer. (b) – SEM micrograph showing the periostracum and the calcite layer without defined microstructure. Bar = 20µm

and internal)[16] which covers the outside of the shells of practically all the molluscs[17]. This layer possesses two principal functions: first, it is the initial support for the first crystals of calcium carbonate, whose nucleation starts at the periostracum inner surface and second, it completely insulates the extrapalial space preventing water intake from the outside environment[18]. The insulation of extrapalial space is essential to the formation of the shell: in this isolated space, the ions responsible for the formation of the precursors of amorphous calcium carbonate (ACC) accumulate, creating a supersaturated solution[17-21], without which biomineralization would not occur. The insulation also enables the animal to control the local pH that alters the solubility of the β-chitin template[22] (nanostructure where the ions are deposited during the heterogeneous nucleation of $CaCO_3$) and activates the mechanism of nucleation.

The Figure 4 (a to f) shows the calcite layer, an irregular polycrystalline massif layer without well-defined morphology, which has been named "Calcite Cloud

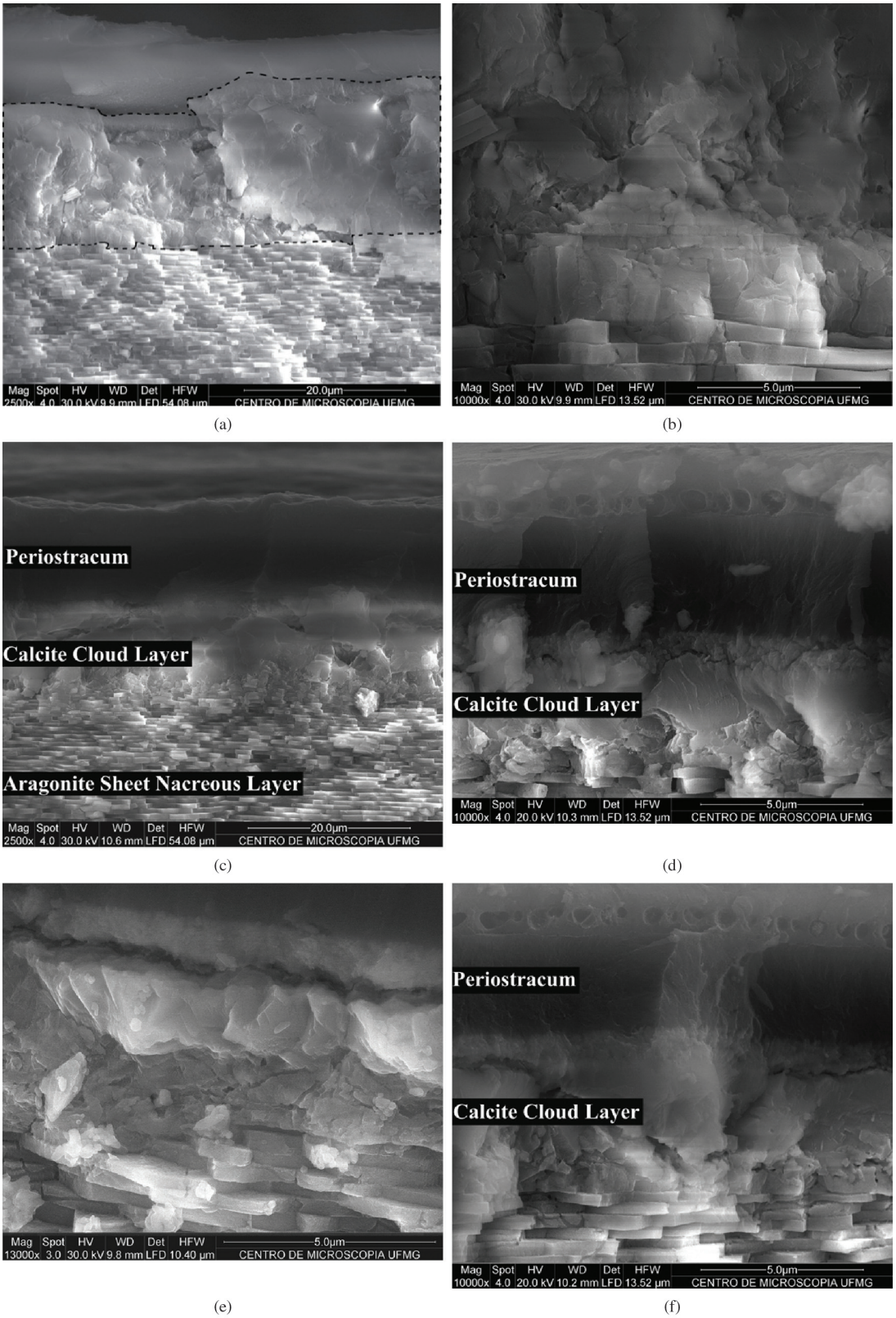

Figure 4. Detail of the calcite layer without defined microstructure; (a) in the upper part is the layer with cloud form composed of calcite (calcite cloud layer – inside the dotted square) and the aragonite sheet nacreous layer; (b) – the calcite cloud layer amplified; (c) – the same layer from another animal and (d) in more detail; (e) and (f) the calcite cloud layer from other specimens denoting the morphology of this layer.

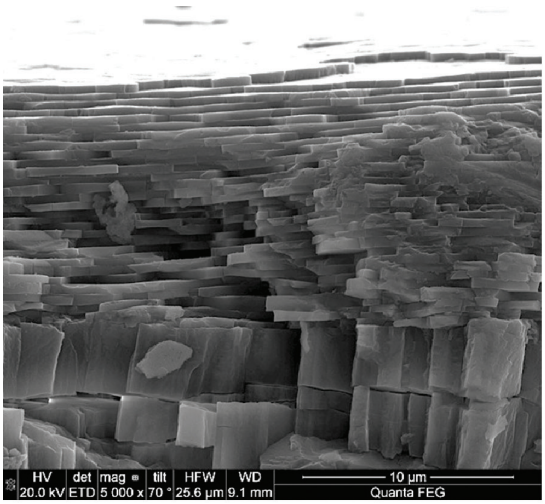

(a)

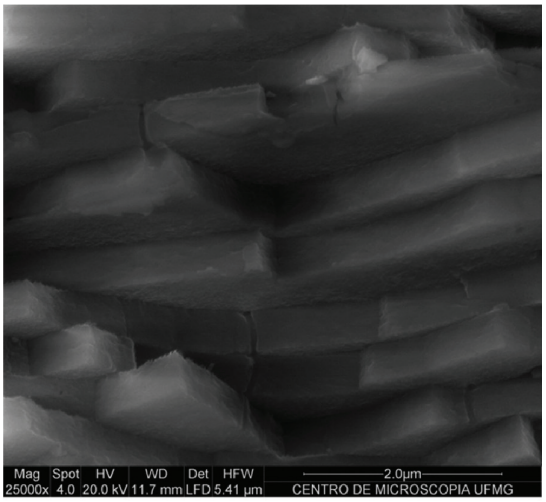

(b)

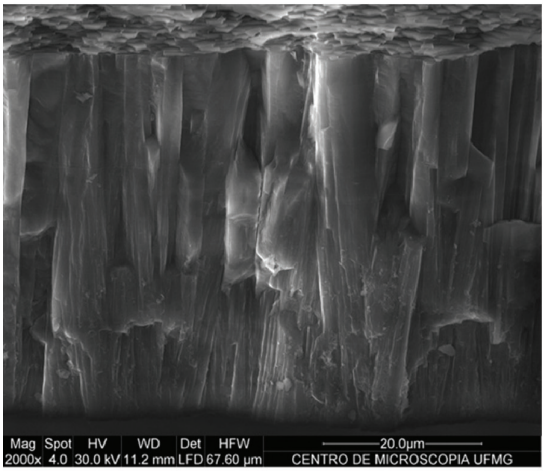

(c)

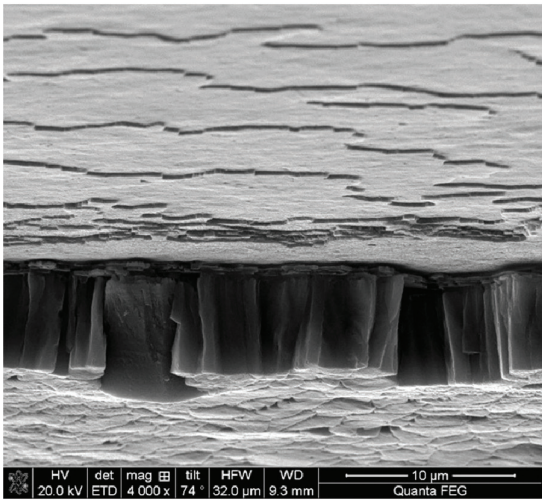

(d)

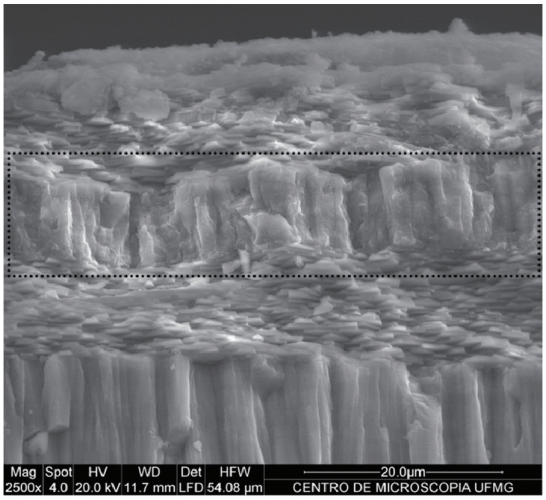

(e)

Figure 5. Scanning electron micrographs. (a) – Sheet nacreous layer composed of aragonite. It makes up the greatest part of the golden mussel shell. Bar = 20µm. (b) – Detailing of overlapping tiles. (c) – Prismatic aragonite layer (internal layer). Bar = 20µm. (d) – Surface view of the intersection between the nacreous layer sheet and the prismatic aragonite layer. Bar = 10µm. (e) – Image showing discontinuous bands growth (mesolayer). Bar = 20µm.

Layer" due to its form remind the nimbus cloud. This is a new microstructure found in the molluscs' shells. The electronmicrographs show in details the morphology of the layer from different animal's shells.

The greater part of the golden mussel's shell structure is constituted of the polymorph aragonite, which is microstructurally organized in the form of superimposed sheets (Figure 5a, b) – the aragonite sheet nacreous layer[6] (≈120μm) – and in the form of prisms (Figure 5c, d) – the aragonite prismatic layer[6] (≈26μm). Contrary to other bivalves[5,7,18,23,24] the prismatic layer in the *L. fortunei* is located in the internal part of the shell and is composed of aragonite. Eventually, along the aragonite sheet nacreous layer, isolated inserts from the prismatic layer can be observed in the form of discontinuous bands (Figure 5e). Known as mesolayers, these inserts are probably related to momentary interruptions in the growth of the sheet nacreous layer, primarily by shortage of the environmental availability of nutrients[17].

3.2. *Atomic force microscopy images*

The AFM images show the topography in three dimensions of the shell of *L. fortunei.* In Figure 6a, the aragonite sheet nacreous layer with the visible fit between the tiles. In Figure 6b, the transition between the sheet nacreous layer and the calcite layer can be observed. In Figure 6c, aragonite prismatic layer, with accentuated topography, immediately follows the end of sheet nacreous layer. In this image, the relatively homogeneous area corresponds to the resin.

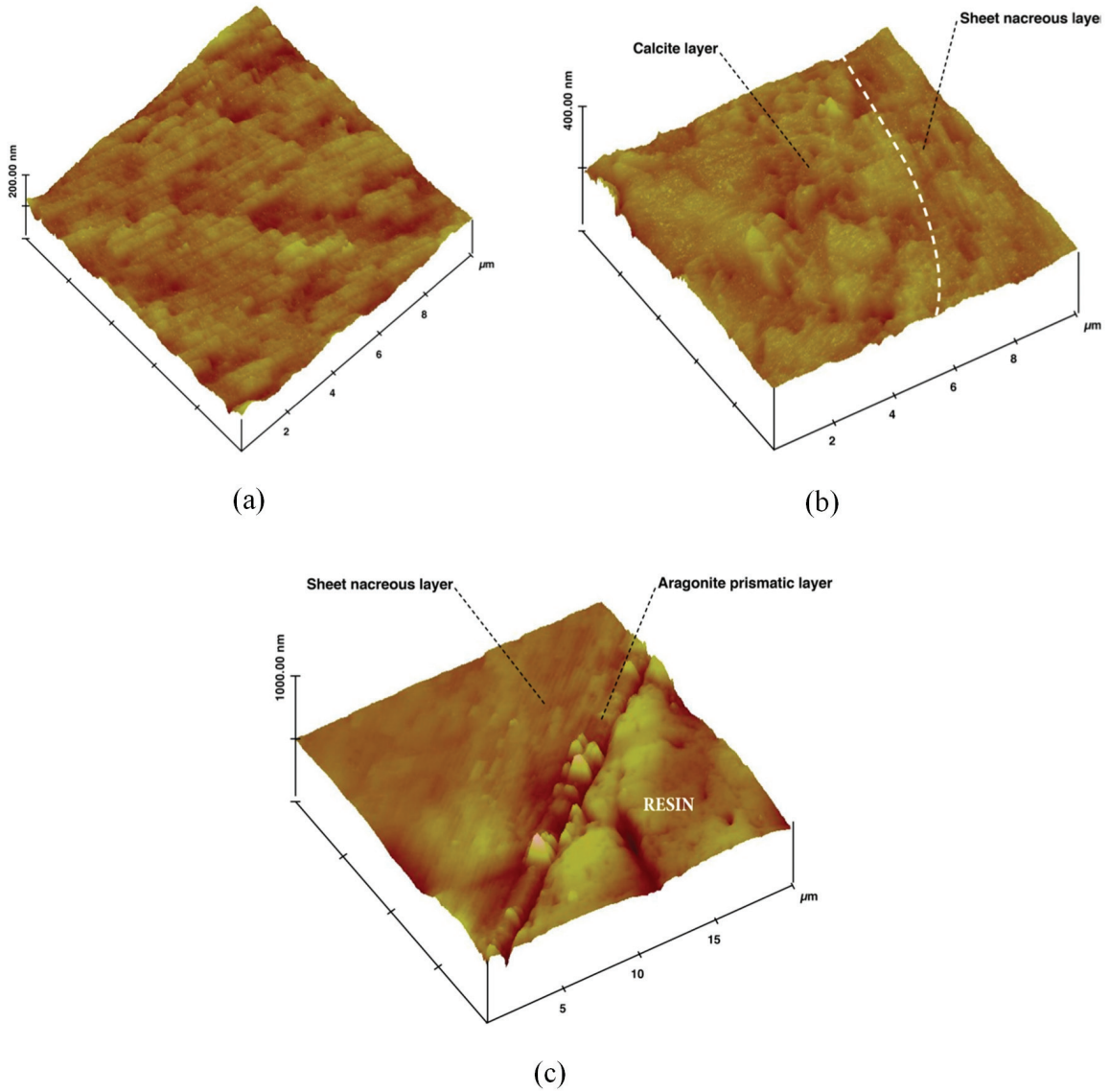

Figure 6. AFM images of a shell layers (a) **–** sheet nacreous layer (b) **–** intersection between the sheet nacreous layer and calcite layer (c) **–** intersection between the sheet nacreous layer and aragonite prismatic layer.

3.3. *X ray diffraction*

In Figure 7 are the diffraction diagrams of the internal regions (a), external dorsal (b), external ventral (c) and of the shell powder (d). In Figure 7a only the intensities corresponding to the aragonite appear, the intensity at 2θ = 31 greater than 2θ = 33.5. In Figure 7b the appearance of the calcite peak (2θ = 29.5) can be seen, albeit with lesser intensity and the presence of the two peaks of the aragonite, which are the same as the internal region of the shell, albeit with lower intensities, which is related to the concentration of this crystalline phase in that region. In Figure 7c is possible to see that the peak of the calcite reaches very high intensity, unlike the other regions and there is only the peak of the aragonite at 2θ = 33.5. The diffraction diagram of the powder (Figure 7d) presents the majority of the peaks of the two polymorphs with different intensities, in addition to the presence of two peaks corresponding to the aragonite (26.5 and 27.5). In this case (diffraction of the whole shell) it should be noted that the aragonite peak at 2θ = 33.5 increases in intensity while that of the calcite peak at 2θ = 29.5 diminishes. The intensities between 85 and 90 (2θ degrees) are preferential orientations that differ from the intensities found at the software card and according to the Figure 7a this orientations correspond to the aragonitic prismatic layer.

4. Conclusions

The polymorph of $CaCO_3$ calcite is present only in the more external ceramic layer (Calcite Cloud Layer) of the shell of *L. fortunei* (below the periostracum). This layer has a microstructure morphologically different from the layers that make up the shells of other bivalves, it does not present a well-defined form as the others do. Despite the apparent absence of morphological pattern in its organization, this layer presents crystalline structure.

The peaks at 2θ = 33.5; 26.55 and 27.55 are associated with the biogenic aragonite, which makes up the aragonite sheet nacreous layer and the intensity at 2θ = 31.0; 85.0 and 88.0 with the biogenic aragonite of the aragonite prismatic layer. There is a greater concentration of calcite in the ventral region of the shell, which may be associated with the mussel's living conditions. The presence of calcite below the periostracum can confirm the hypothesis[19] that the biomineralization of aragonite mesocrystals (forming the aragonite sheet nacreous layer and aragonite prismatic layer) need a previously mineralized layer supporting the

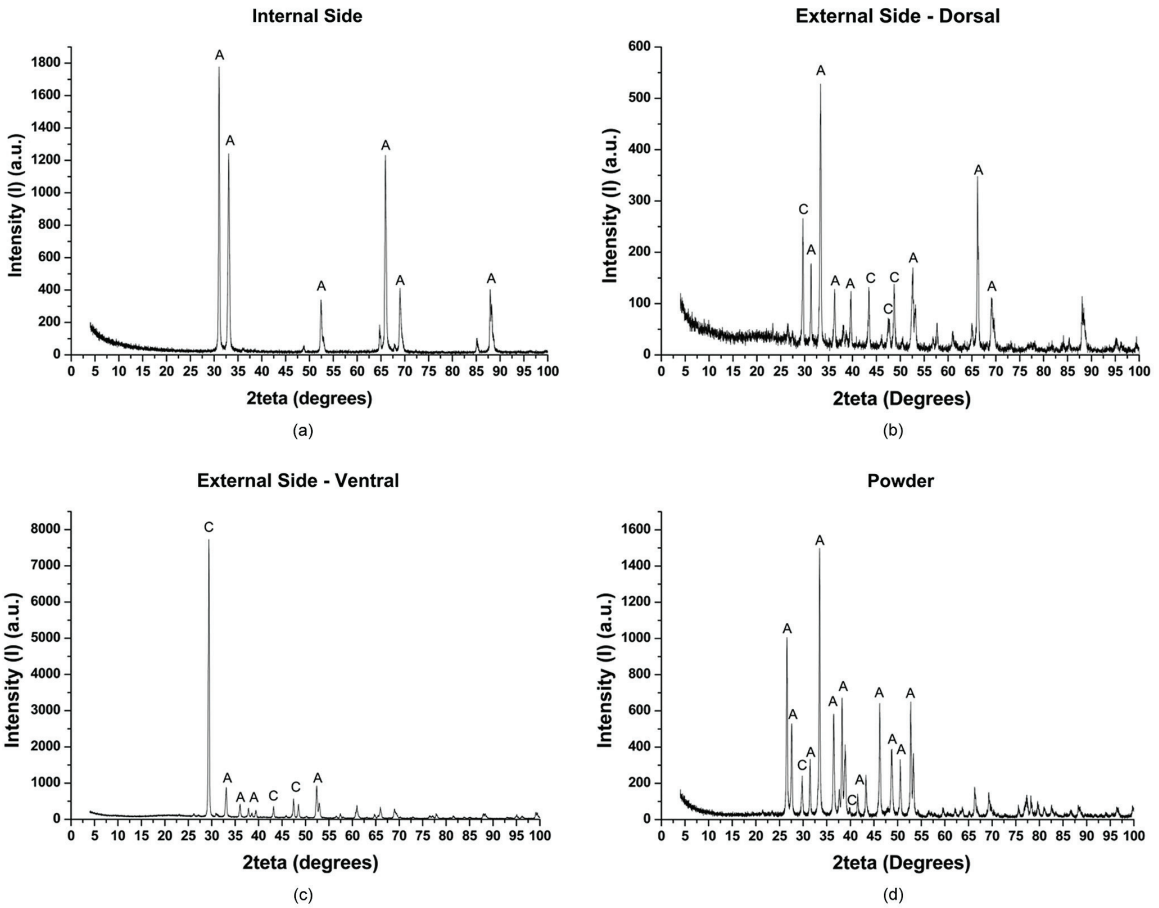

Figure 7. Diffraction patterns obtained from the internal regions (a), external dorsal (b), external ventral (c) and of the shell powder (d) of the golden mussel. A – Aragonite intensities and C – Calcite intensities.

organic matrix that, through their chemical and structural singularities (such as micro and nanoporosities and presence of channels) provides stability to aragonite, ensuring the structural hierarchy of tiles and prisms.

Acknowledgements

Our thanks go to CEMIG – *Geração e Transmissão* for the financial support (Project GT 343 – Control of the golden mussel: bioengineering and new materials for application in ecosystems and hydropower plants); to José Mário Carneiro Vilela – CETEC-SENAI for AFM images acquisition; to REDEMAT UFOP-UEMG-CETEC for the institutional support; to the Centre of Microscopy of the Universidade Federal de Minas Gerais (http://www.microscopia.ufmg.br) for providing the equipment and technical support for experiments involving electron microscopy.

References

1. Joseph RS. The crystal structure of calcite III. *Geophysical Research Letters*. 1997; 24(13):1595-1598. http://dx.doi.org/10.1029/97GL01603
2. Fiona CM and Helmut C. Controlling Mineral Morphologies and Structures in Biological and Synthetic Systems. *Chemical Reviews*. 2008; 108:4332-4432. http://dx.doi.org/10.1021/cr8002856
3. Weiner S and Addadi L. Crystallization Pathways in Biomineralization. *Annual* Review *of Materials Research.* 2011; 41: 21-40. http://dx.doi.org/10.1146/annurev-matsci-062910-095803
4. Fricke M and Volkmer D. *Crystallization of calcium carbonate beneath insoluble monolayers*: suitable models of mineral-matrix interactions in biomineralization? Topics in Current Chemistry. 2007; 207:1-41. http://dx.doi.org/10.1007/128_063
5. Gosling EM. *Bivalve Molluscs*. Wiley-Blackwell; 2003.
6. Kobayashi I and Samata T. Bivalve Shell Structure and Organiz Matrix. *Material Science and Engeneering C*. 2006; 26:692-698. http://dx.doi.org/10.1016/j.msec.2005.09.101
7. Lopes-Lima M, Rocha A, Gonçalves F, Andrade J and Machado J. Microstructural Characterization of inner Shell Layers in the Freshwater Bivalve *Anodontacygnea. Journal of Shellfish*. 2010; 29(4):969-973. http://dx.doi.org/10.2983/035.029.0431
8. Lin A and Meyers MA. Growth and Structure in Abalone Shell. *Materials Science and Engineering A*. 2005; 390:27-41. http://dx.doi.org/10.1016/j.msea.2004.06.072
9. Taylor JD and Layman M. The Mechanical Properties of Bivalve (Mollusca) Shell Structures. *Paleontology*. 1972; 15:73-87.
10. Yang W, Kashani N, Li X-W, Zhang G-P and Meyers MA. Structural Characterization and Mechanical Behavior of a Bivalve Shell (*Saxidomus purpuratus*). *Materials Science & Engineering: C*. 2011; 31(4):724-729. http://dx.doi.org/10.1016/j.msec.2010.10.003
11. Barthelat F. Nacre from Mollusk Shells: A Model for High-Performance Structural Materials. *Bioinspiration & Biomimetics*. 2010; 5(3). http://dx.doi.org/10.1088/1748-3182/5/3/035001
12. Yang W, Zhang GP, Zhu XF, Li XW and Meyers MA. Structure and Mechanical Properties of *Saxidomus purpuratus* biological shells. *Journal of the Mechanical Behavior of Biomedical Materials.* 2011; 4(7):1514-1530. http://dx.doi.org/10.1016/j.jmbbm.2011.05.021
13. Avelar W, Martim S and Vianna MP. A New Occurrence of *Limnoperna fortunei* (Dunker 1856) (Bivalvia, Mytilidae) in the State of São Paulo. *Brazilian Journal of Biology*. 2004:793-742.
14. Spaccesi FG and Rodrigues Capitulo A. Benthic Communities on Hard Substrates Covered by *Limnoperna fortunei* Dunker (Bivalvia, Mytilidade) at an Estuarine Beach (Río de la Plata, Argentina). *Journal of Limnology.* 2012; 71(1):144-153. http://dx.doi.org/10.4081/jlimnol.2012.e15
15. Pareschi DC, Matsumura-Tundisi T, Medeiros GR, Luzia AP and Tundisi JG. First Occurance of *Limnoperna fortunei* (Dunker, 1857) in Rio Tietê Watershed (São Paulo State, Brazil). *Brazilian Journal of Biology.* 2008; 68(4): 1107-1114. http://dx.doi.org/10.1590/S1519-69842008000500017
16. Checa A. A New Model for Periostracum and Shell Formation in Unionidae (Bivalvia, Mollusca). *Tissue & Cell.* 2000; 32(5):405-416.
17. Harper E. The Molluscan Periostracum: An Important Constraint in Bivalve Evolution. *Paleontology*. 1977; (40):71-97.
18. Marin F and Luquet G. Molluscan Shell Proteins. *Comptes Rendus Palevol*. 2004: 3(6-7):469-492. http://dx.doi.org/10.1016/j.crpv.2004.07.009
19. Saruwatari K, Matsui T, Mukai H, Nagasawa H and Kogure T. Nucleation and growth of aragonite crystals at the growth front of nacres in pearl oyster, *Pinctada fucata*. *Biomaterials*. 2009; 30(16):3028-3034. http://dx.doi.org/10.1016/j.biomaterials.2009.03.011
20. Meyers MA, Chen P-Y, Lin A Y-M and Seki Y. Biological materials: Structure and mechanical properties. *Progress in Materials Science*. 2008; 53(1):1-206. http://dx.doi.org/10.1016/j.pmatsci.2007.05.002
21. Akella K. Biomimetic Designs Inspired by Seashells. *Resonance.* 2012; 17(6):573-591. http://dx.doi.org/10.1007/s12045-012-0063-2
22. Xiao J and Yang S. Biomimetic Synthesis, Hierarchical Assembly and Mechanical Properties of Calcite/Chitosan Composites in a Three-Dimensional Chitosan Scaffold. *Advanced Engineering Materials.* 2011; 13(1-2):B32-B40. http://dx.doi.org/10.1002/adem.201080068
23. Kobayashi I. Internal Microstructure of the Shell of Bivalve Molluscs. *Integrative and Comparative Biology*. 1969; 9(3):663-672. http://dx.doi.org/10.1093/icb/9.3.663
24. Jacob DE, Soldati AL, Wirth R, Huth J, Wehrmeisterd U and Hofmeister W. Nanostructure, composition and mechanisms of bivalve shell growth. *Geochimica et Cosmochimica Acta*. 2008; 72(22):5401-5415. http://dx.doi.org/10.1016/j.gca.2008.08.019